RSC Advances

PAPER

View Article Online
View Journal | View Issue

Check for updates

Cite this: *RSC Adv.*, 2025, **15**, 51110

Discovering a green pesticide candidate for controlling bacterial plant disease: 1,2,3,4-tetrahydro-β-carboline as a potential biofilm inhibitor

Puying Qi, *[ad] Hongwu Liu,[b] Yue Li,[a] Daiyu Tang,[c] Lei Shao,[a] Junjie Wang,[ad] Qifei Zhu,[a] Taibai Jiang,[a] Lixia Li,[a] Shilong Jiang,[a] Fan Wu,[a] Yanhong Guo,[a] Yong Liu,[a] Lihong Shi,*[a] Yin Wang*[a] and Jun Sun*[ef]

Received 3rd October 2025
Accepted 6th December 2025

DOI: 10.1039/d5ra07526b

rsc.li/rsc-advances

Xanthomonas oryzae pv. *Oryzae*, result in rice bacterial blight, is the most severe bacterial disease affecting rice, and in certain regions, it is considered the most critical disease overall, with the potential to reduce yields by as much as 50%. It is difficult to control rice bacterial blight and lacking of pesticides. 1,2,3,4-Tetrahydro-β-carboline (THC) and their analogues show a diverse range of activities; however, research specifically focusing on THC remains limited, particularly concerning its antibacterial properties. Given its promising characteristics, THC holds potential for development as an environmentally friendly green pesticide. These outcomes reveal that THC signally inhibits both the cell growth and biofilm formation, thereby reducing its pathogenicity. Consequently, THC holds promise as a novel green pesticide aimed at targeting bacterial biofilms to effectively manage rice bacterial leaf blight.

1. Introduction

Alkaloids, along with 1,2,3,4-tetrahydro-β-carboline (THC) and their analogues, show a broad spectrum of activities, including antiviral,[1] antitumor,[2] antibacterial,[3] antifungal,[4] anti-inflammatory,[5] antioxidant,[6] and insecticidal effects.[7] Most researches have predominantly focused on THC derivatives, while research on THC itself, particularly its antibacterial effects, remains relatively scarce. In our prior study,[8] it was demonstrated that THC displayed favorable anti-bacterial activity against bacterial blight of rice, with an EC_{50} value of 16.27 μg mL^{-1}. Nevertheless, the potential anti-bacterial mechanism of THC against *Xoo* and its *in vivo* control efficacy have not been comprehensively investigated. Bacterial blight is a rice bacterial disease triggered by *Xoo*.[9,10] When this disease occurs, it is challenging to manage, and currently, there is a lack of effective bactericides for controlling rice bacterial blight. The carboline alkaloid THC possesses the biocompatibility attributes characteristic of natural products, suggesting its potential for development as a green pesticide.[11,12] Published researches have shown that carbolines have antibacterial effects on bacterial biofilms. However, more in-depth investigations into the underlying mechanisms are still lacking. Biofilm is an organized assembly of bacteria that adheres to the surfaces of either living or non-living objects, encased in extracellular macromolecules produced by the bacteria and the formation process of biofilms showed in Fig. 1.[13,14] Biofilm bacteria are highly resistant to antibiotics and host immune defense mechanisms.[15,16] There are various major biological macromolecules such as proteins, extracellular polysaccharides, DNA, RNA, peptidoglycan, phospholipids and other substances in the biofilm.[17,18] Biofilm formation is a dynamic process, including the incipient adhesion, colonization, biofilms development and mature diffusion of bacteria.[19] *Reversible adhesion stage*: planktonic microorganisms (such as bacteria) contact with the surface of the object through flagella, cilia or pili, forming a reversible temporary adhesion.[20,21] At this time, the microorganism is only wrapped by a small amount of extracellular polymer, and may still re-enter the planktonic state.[22] *Irreversible adhesion stage*: by regulating gene expression (such as activating biofilm-related genes), microorganisms secrete a large number of extracellular polymers (such as extracellular polysaccharides, EPS), enhance adhesion to the surface, and enter an irreversible

[a]*Guizhou Province Engineering Research Center of Medical Resourceful Healthcare Products, College of Pharmacy, Guiyang Healthcare Vocational University, Guiyang, 550081, China. E-mail: qpuying000@163.com; qipuying@gyhvu.edu.cn; shilihong@zju.edu.cn; ada_wy@126.com*

[b]*National Key Laboratory of Green Pesticide, Key Laboratory of Green Pesticide and Agricultural Bioengineering, Ministry of Education, Center for R&D of Fine Chemicals of Guizhou University, Guiyang, 550025, China*

[c]*Guizhou Provincial Center for Disease Control and Prevention, Guiyang, 550004, China*

[d]*Guizhou Provincial Doctor Innovation Station, Southeastern, Guizhou Province, 556400, China*

[e]*College of Chemistry and Chemical Engineering, Guizhou University of Engineering Science, Xueyuan Road, Qixingguan District, Bijie 551700, China*

[f]*Analytical and Testing Center, Guizhou University of Engineering Science, Xueyuan Road, Qixingguan District, Bijie 551700, China. E-mail: sunjun@gues.edu.cn*

Open Access Article. Published on 24 December 2025. Downloaded on 2/3/2026 5:24:52 AM.
This article is licensed under a Creative Commons Attribution-NonCommercial 3.0 Unported Licence.

© 2025 The Author(s). Published by the Royal Society of Chemistry

Open Access Article. Published on 24 December 2025. Downloaded on 2/3/2026 5:24:52 AM.
This article is licensed under a Creative Commons Attribution-NonCommercial 3.0 Unported Licence.

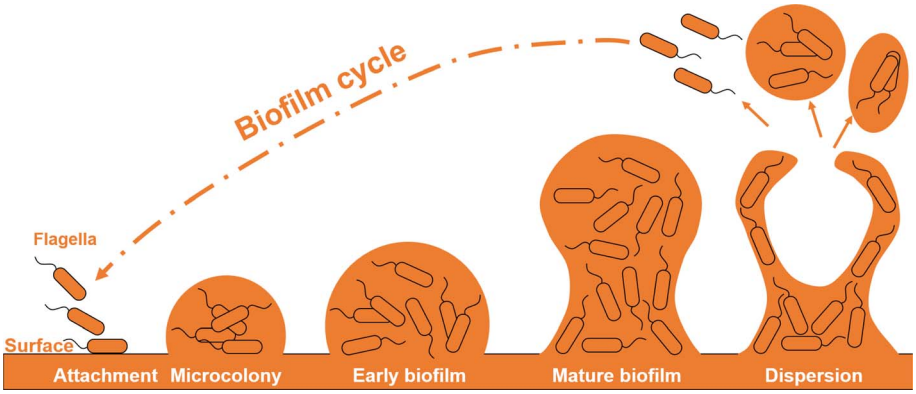

Fig. 1 The formation and cycle of bacterial biofilm.

fixed state.[23,24] The hydrogel matrix formed by EPS provides protection for subsequent colonies.[25] *The formation and maturation stage of the colony*: the adhered microorganisms form microcolonies by division and proliferation, and secrete more extracellular polymers (EPS) to cover the surface to form hydrogel-like EPS, and gradually construct a three-dimensional biofilm structure.[19,26] The mature biofilm presents a "mushroom-like" or "pile-like" micro-colony group, and a channel network is formed inside to transport nutrients and metabolic waste, similar to the original circulatory system.[27,28] At this stage, the biofilm thickness can reach tens of microns, and the dissolved oxygen consumption is significantly increased.[29,30] *The shedding and recolonization stage*: due to the internal anaerobic metabolic gas production or external erosion of the mature biofilm, part of the shedding releases planktonic microorganisms, which can recolonize to form new biofilms and complete the cycle.[31,32] The EPS matrix provides a physical barrier and significantly enhances the tolerance of the biofilm to disinfectants, ultraviolet rays, antibiotics and temperature.[33,34] Therefore, this study aims to conduct an in-depth exploration of THC against *Xoo*, thereby providing valuable insights for the discovery of novel green pesticides.

2. Materials and methods

2.1. Instruments and chemicals

The sterilized six well plate, ninety-six well plate, and crystal violet (purity, 2.5%) was obtained from BKMAM Biotech Technology Co., Ltd, Changde city, Hunan Province, China. The dimethylsulfoxide (DMSO, >99.8%, GC), and 1,2,3,4-Tetrahydro-β-carboline (THC, 96%) were purchased from Shanghai Aladdin Biochemical Technology Co., Ltd, China. Orange peel essential oil (OPO) was purchased from Henan Moore Water soluble Fertilizer Co., Ltd. The assessment of fluorescence imaging of *Xoo* was performed using Olympus-BX53 microsystem (Japan). The contact angle was measured using POWEREACH contact angle instrument, Shanghai, China.

2.2. MIC value of THC against *Xoo*

The MIC value assessment of THC against *Xoo* was performed according to our published work.[35]

2.3. Crystal violet and acridine orange staining assay of bacterial biofilm

2.3.1. Crystal violet staining biofilm. The 5 mL liquid bacterial medium was added to 15 mL glass test tubes and the THC working solution (10 μL, 0.05 mg μL^{-1}) was added to tubes to a final concentration of 100 μg mL^{-1}. The dimethyl sulfoxide was added as control (0 μg mL^{-1}). 40 μL *Xoo*-suspension was added to tubes. All treatment were statically cultured at 28 °C for 72 hours. Glass test tubes were stained with 1% crystal violet solution for 15 min. OD_{490} values were measured at 490 nm to assess the biofilm inhibition rate.

2.3.2. Acridine orange staining biofilms. The OD_{595nm} value of *Xoo* cell suspension was adjusted to 0.1. Then, liquid cell suspension (4 mL) was added to the sterile polystyrene six well plate. However, the THC working solution (8 μL, 0.05 mg μL^{-1}) was poured into six well plate forming an ultimate density of 100 mg L^{-1}. Dimethyl sulfoxide was added as control (0 μg mL^{-1}). Subsequently, a small and sterile glass sheet was placed in all well. Six well plates were sealed and cultured in the constant temperature incubator at 28 °C for 72 hours. Then, each glass sheet was stained using acridine orange dye.[36] Finally, all data was analysed using software and an Olympus-BX53 microsystem.

2.4. Bacterial motility assay

Firstly, the heated 4 mL semisolid medium including 0.5% agar was poured into a six well plates. Then, THC were added to every well to obtain the mixture solutions with various of doses of 0 and 100 μg mL^{-1}. Next, 2 μL bacterial *Xoo* suspension was poured into the middle of six well plates after cooling and forming a semisolid medium. The six well plates containing medium, cells suspension, and THC were placed and co-cultured in a constant temperature incubator at 28 °C for seventy-two hours. Finally, the bacterial motility diameter was detected.[37]

2.5. The assay of bacterial pathogenicity

Firstly, 40 μL THC and 40 μL thiadiazole-copper (TC) working solution was poured into 20 mL liquid-medium respectively to obtain the mixed solutions with various of doses and 100 μg

Open Access Article. Published on 24 December 2025. Downloaded on 2/3/2026 5:24:52 AM. This article is licensed under a Creative Commons Attribution-NonCommercial 3.0 Unported Licence.

mL^{-1}. 40 μL DMSO was poured into 20 mL medium to obtain the solutions with various of doses 0 μg mL^{-1}. Secondly, 160 μL *Xoo*-suspension was added to 20 mL liquid medium and the mix-medium were incubated for 72 hours in an incubator at 28 °C. Then, OD_{595} values of every treatment are adjusted to 0.5. Rice leaves at tillering stage were inoculated with a bacterial suspension ($OD_{595} = 0.5$). Meanwhile, rice was cultured at 28 °C in 80% humidity in an artificial climate incubator. Lastly, all leaves lesion length were measured and calculated.[38]

2.6. Controlling rice bacterial leaf blight at *in vivo* level

Rice leaves at tillering stage were inoculated with a *Xoo* cells suspension for culturing 24 hours at 28 °C in 80% humidity in an artificial climate incubator. Then, THC and TC working solutions (200 mg L^{-1}) were applied to the rice leaf. Rice was cultured 14 days in an artificial climate incubator and leaves lesion length were measured and morbidity, disease index, control efficiency was calculated.[39]

2.7. Orange peel essential oil (OPO) improving the control effective *in vivo*

0.3% OPO was added into THC to improving the control effective *in vivo* against rice bacterial leaf blight. Experimental method referred to the experimental procedure of 2.6.[40]

2.8. ADMET evaluation and phytotoxicity

The evaluation of ADMET was performed using the software of ADMETlab 2.0.[41] The SMILES of THC were submitted into "https://admetmesh.scbdd.com/service/evaluation/index". Lastly, these outcomes were shown in a Table S1.

2.9. Statistical analysis

Every treatment was performed for three times. Using ANOVA method to assess the differences between every treatment (Origin 2021, Origin Company, USA). All experimental data was showed in figures (*) $p < 0.05$, (**) $p < 0.01$, (***) $p < 0.001$ *vs.* control or 0 μg mL^{-1}.

3. Results and discussion

3.1. THC inhibits the growth of *Xoo*

It has been found that bacterial biofilms can be used as a potential molecular target for drug discovery.[42] The strategy of targeting biofilm is to affect only the formation of biofilms without impacting on the normal bacteria, thus reducing the pathogenicity and bacterial virulence to achieve the purpose of preventing and controlling bacterial diseases.[43] Therefore, targeting bacterial biofilm is a promising antimicrobial strategy.[44] Some studies have found that β-carbolines exhibited an antibacterial biofilm activity.[45] According to the published work, we found that THC exhibited fine antibacterial activity against bacteria, however, the underlying antibacterial mechanism was not investigated.[8] Therefore, in our current study we discussed in depth the mechanism of THC against *Xoo*. Table 1 and Fig. 2 show the chemical structural formula and MIC value of THC,

Table 1 The inhibition ratio of THC against *Xoo* at the concentrations of 100, 125, and 150 μg mL^{-1}, and TC against *Xoo* at the concentrations of 500 μg mL^{-1}

Treatment	Concentrations (μg mL^{-1})	Inhibition ratio (%)
THC	150	100 ± 0.01
	125	37.52 ± 6.46
	100	7.56 ± 11.16
Thiodiazole-copper (TC)	500	0

the results of which showed that THC inhibited *Xoo* by 100 ± 0.01%, 37.52 ± 6.46%, and 7.56 ± 11.16% at the action concentrations of 150, 125, and 100 μg mL^{-1}, respectively. Thus, it is seen that THC significantly inhibited the growth and proliferation of *Xoo* at the action concentrations of 150 and 125 μg mL^{-1}, especially at 150 μg mL^{-1}, the bacteria almost stopped growing and proliferating. The inhibition rate of thiadiazole-copper against *Xoo* was 0 at the concentration of 500 μg mL^{-1}. It can be seen that the MIC value of THC is 150 μg mL^{-1}. MIC value of thiodiazole copper is more than 500 μg mL^{-1}. Although THC still showed some inhibitory effect at an action concentration of 100 μg mL^{-1}, it almost had no effect on the growth and proliferation of the bacteria. Therefore, THC can be used as a potential *Xoo* biofilm-targeting inhibitor if it achieves only inhibition of biofilm formation without affecting bacterial growth and proliferation at an action concentration of 100 μg mL^{-1}. Therefore, we choose 100 μg mL^{-1} as the drug action concentration in the subsequent study. In addition, we purchased four THC analogues and evaluated their antibacterial activity. As shown in Fig. S1 and 2, the results show that only compound 6-methoxy-1,2,3,4-tetrahydro-β-carboline displayed certain anti-*Xoo* activity, and the MIC value is 300 μg mL^{-1}, which is much lower than the antibacterial activity of THC. Other compounds have almost no antibacterial activity at concentrations of 50–500. Thereby, THC might be a potential pesticide candidate for controlling plant disease.

3.2. The assay of biofilm formation

Biofilms play an extremely significant role in bacterial pathogenesis,[46] and more than 65–80% of microbiological contamination worldwide is closely associated with biofilm,[47] which are also secreted by phytobacteria to promote bacterial pathogenicity when infecting host plant cells.[48] Moreover, β-carbolines have a certain inhibitory effect on biofilms.[49] Therefore, this study investigated the effect of THC on *Xoo* biofilm. Crystalline violet can stain the biofilm to quantify the biofilm.[50] These results of the crystalline violet staining experiments in Fig. 3A and B showed that the inhibition rate of THC on *Xoo* biofilm was 60.89% at 100 μg mL^{-1} action concentration, which significantly inhibited the formation of biofilm. It was further found that acridine orange could fluorescently stain bacteria in the biofilm state, thus visualizing the effect of *Xoo* biofilm by THC. The results of fluorescence staining experiments showed that the green fluorescence intensity of the bacteria at 100 μg

© 2025 The Author(s). Published by the Royal Society of Chemistry

Open Access Article. Published on 24 December 2025. Downloaded on 2/3/2026 5:24:52 AM.
This article is licensed under a Creative Commons Attribution-NonCommercial 3.0 Unported Licence.

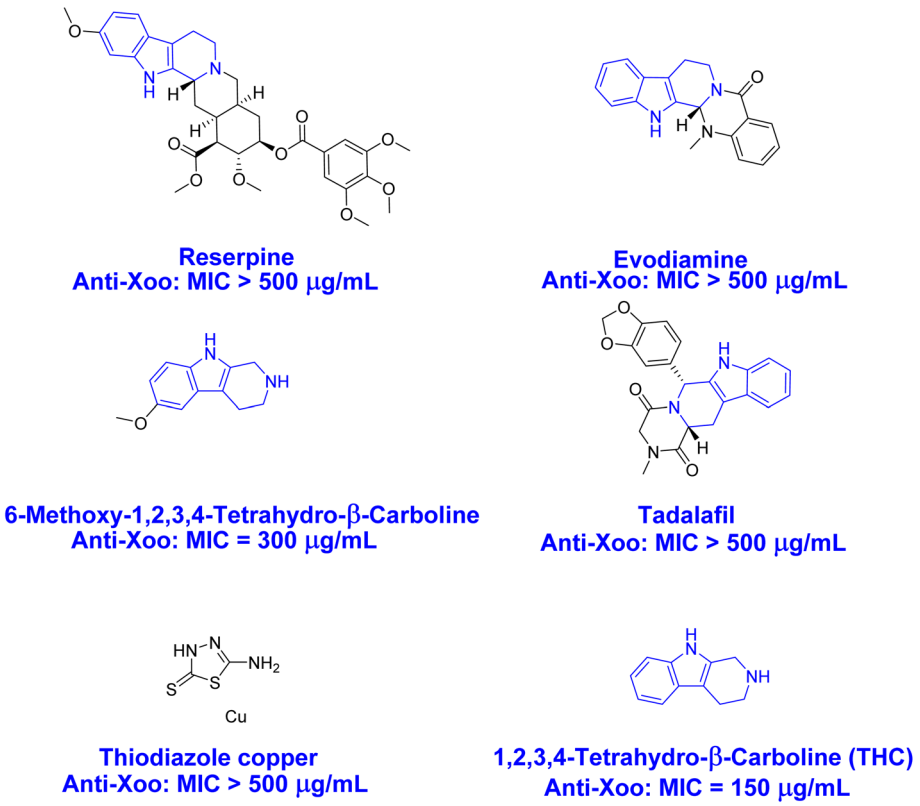

Fig. 2 The chemical structural formula and MIC value of THC analogues and thiodiazole copper.

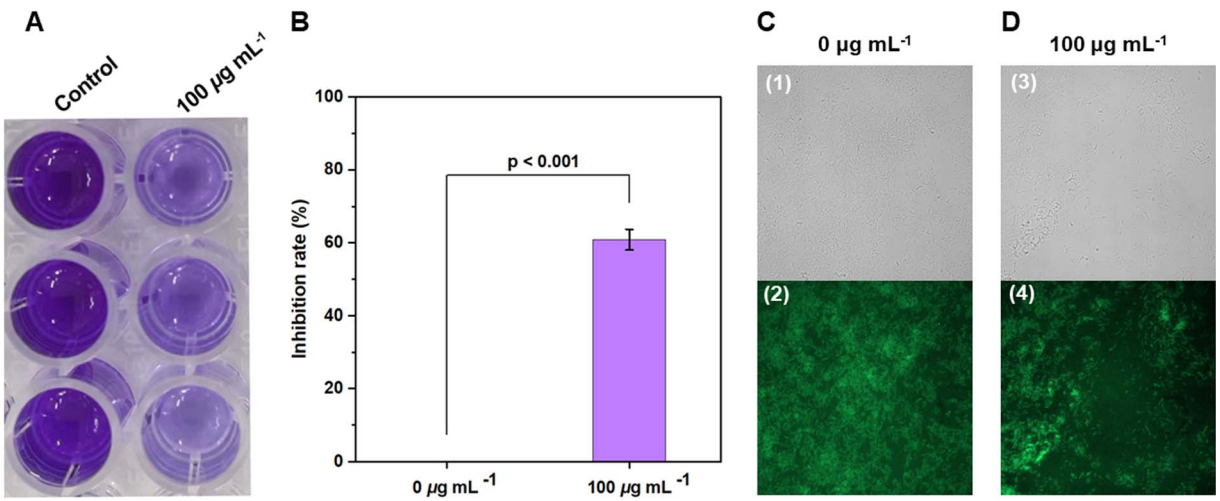

Fig. 3 *Xoo*-biofilm inhibition. (A and B) Crystal violet staining showing *Xoo*-biofilm inhibition at 490 nm (OD_{490nm}) after treatment with THC (0 and 100 μg mL^{-1}). (C and D) Acridine orange staining bacterial biofilm at the concentration of 0 and 100 μg mL^{-1}. Every treatment was performed for three times.

mL^{-1} action concentration of THC was 55.36, while the fluorescence intensity (calculating fluorescence intensity with Image J software) of the control group was 81.97, which showed that THC could significantly inhibit the formation of biofilms, interfere with the pathogenic process of the bacteria, and reduce the pathogenicity (see Fig. 3C and D).

3.3. The assay of motility

Most bacteria have good motility and mobility is one of the fastest movement modes of bacteria.[51,52] It enables bacteria to sense environmental changes, avoid harmful environmental stimuli, and move to nutrient-rich environments, which ultimately significantly improves their environmental adaptability

Open Access Article. Published on 24 December 2025. Downloaded on 2/3/2026 5:24:52 AM.
This article is licensed under a Creative Commons Attribution-NonCommercial 3.0 Unported Licence.

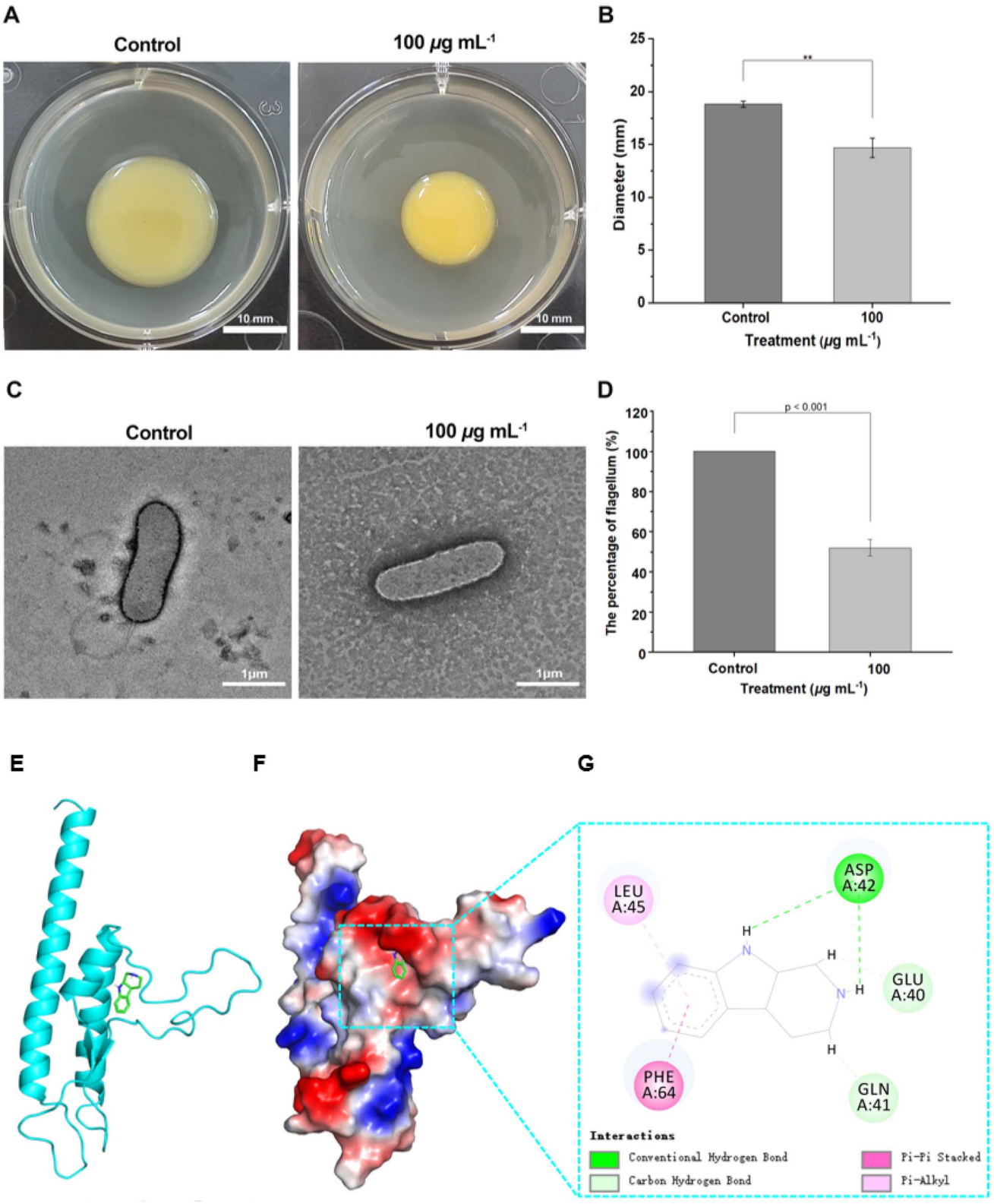

Fig. 4 The effect of THC on bacterial motility. (A) Motility plate analysis of *Xoo*, treated with DMSO (control), and THC (100 μg mL^{-1}). (B) The inhibition ratio of *Xoo*-motility treated with DMSO and THC. (**) $p < 0.01$. Scale bars are 10 mm. (C) TEM monitoring the morphological changes of *Xoo*-flagellum after treatment with THC (DMSO, serve as control), and 100 μg mL^{-1}. (D) The percentage of *Xoo*-flagellum. Scale bars = 1 μm. The binding mode of FlgB with THC. (E) The 3D structure of complex. (F) The electrostatic surface of FlgB protein. (G) The detail binding mode of complex. Every treatment was performed for three times.

© 2025 The Author(s). Published by the Royal Society of Chemistry

Open Access Article. Published on 24 December 2025. Downloaded on 2/3/2026 5:24:52 AM.
This article is licensed under a Creative Commons Attribution-NonCommercial 3.0 Unported Licence.

and pathogenicity.[53] The results of the bacterial motility experiments in Fig. 4A and B showed that the natural alkaloid THC at a concentration of 100 μg mL^{-1} had a significant inhibitory effect on the motility of *B. albicans* at 14.7 mm and 18.8 mm in the control group. The bacterial flagellum had a significant inhibitory effect on the motility, and its diameter was 14.7 mm and 18.8 mm in the control group, respectively.[54] The swimming diameter was 14.7 mm, while that of the control group was 18.8 mm. Bacterial flagellum is an important locomotor organ responsible for bacterial mobility, and usually the flagellum is composed of three parts: flagellar filament, flagellar hook and matrix. The movement of bacterial cells towards beneficial environments and avoidance of harmful environments, as well as the flagellum-mediated swimming play an important role in the bacterial infestation cycle, which undoubtedly increases the probability of cell colonization of the host plant surface. This ability enhances the efficiency of bacterial search and enables the bacteria to avoid harm. This suggests that bacterial virulence to the host is significantly influenced by flagellum-mediated movement. As shown in Fig. 4C and D, the percentage of flagellar self-assembly was 100% and 52% at 0 and 100 μg mL^{-1} action concentrations, respectively. These results suggest that compound THC strongly interfered with the flagellar self-assembly process and caused a decrease in bacterial virulence at an action concentration of 100 μg mL^{-1}. The rice leaf blight bacterium in this study is a unipolar flagellated bacterium, and the synthesis of flagella depends on regulatory proteins such as FlgB, which is involved in pathogenic processes such as bacterial motility, chemotaxis, and biofilm formation, and promotes the attachment and spread of pathogenic bacteria to host tissues at the early stage of infection; therefore, inactivation of the FlgB protein can lead to a complete absence of the flagellum, which affects bacterial motility and virulence. Therefore, based on the above experimental results, this study further investigated the effect of THC on bacterial flagellar self-assembly. As shown in Fig. 4E–G, the molecular docking results showed that THC existed and well-matched with FlgB protein, with a binding energy of −6.85 kcal mol^{-1}. The binding mode results indicated that THC could form two hydrogen bond interactions with FlgB protein residue ASP-42, with a strong binding ability, which was important for anchoring small molecules in the protein pocket; in addition, THC could also interact with LEU-42, which was the most important molecule in the protein pocket. In addition, THC can also form hydrophobic interactions with LEU-45, PHE-64, and the benzene ring in the molecular structure of THC can also form pi–pi conjugation interactions with PHE-64 residues, all of which are important for stabilizing small molecules. These interactions can promote the formation of stable complexes between THC and FlgB proteins, which are highly protein-associated. Taken together, THC may inhibit flagellar biosynthesis by interacting with FlgB proteins leading to

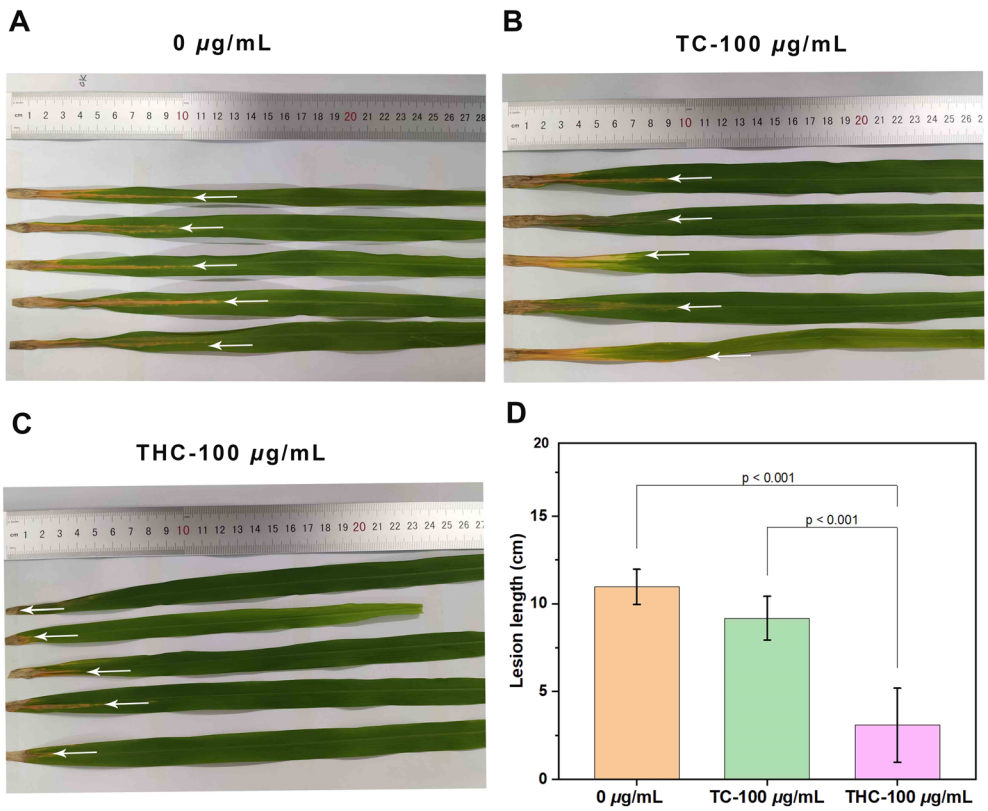

Fig. 5 The effect of THC and TC on the pathogenicity of *Xoo*. Pathogenicity analysis of rice leaves following treatment with different doses of (A) 0 μg mL^{-1} (DMSO), (B) TC (100 μg mL^{-1}), and (C) THC (100 μg mL^{-1}) for 14 days. (D) The lesion length of rice leaves after treating with DMSO, TC, and THC. Every treatment was performed for three times.

© 2025 The Author(s). Published by the Royal Society of Chemistry

Open Access Article. Published on 24 December 2025. Downloaded on 2/3/2026 5:24:52 AM.
This article is licensed under a Creative Commons Attribution-NonCommercial 3.0 Unported Licence.

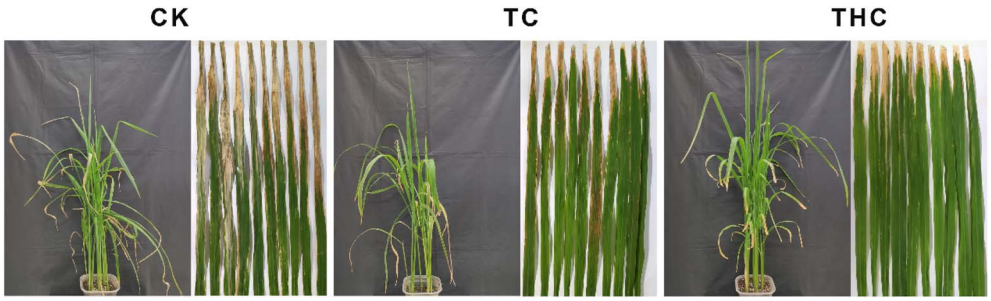

Fig. 6 The curative activity of TC and THC against *Xoo* at 0 μg mL^{-1} (served as CK), TC-200 μg mL^{-1}, and THC-200 μg mL^{-1}.

Table 2 Curative activity of THC and TC against *Xoo* under greenhouse conditions at 200 μg mL^{-1} *in vivo*

	Curative activity		
Treatment	Morbidity	Disease index	Control efficiency[b]
THC	100%	60.0%	32.5%
TC	100%	62.2%	30.0%
CK[a]	100%	88.9%	—

[a] Control. [b] Statistical analysis was performed using ANOVA under condition of equal variances assumed ($p < 0.05$).

reduced bacterial mobility and thus attenuating bacterial pathogenicity.

3.4. The assay of pathogenicity

Pathogenic bacteria use virulence factors to overcome host defenses,[55] and many virulence factors are closely associated with infections caused by bacteria. Bacterial biofilms, motility, flagella, and other virulence factors are critical facilitating bacterial colonization and enhancing pathogenicity during infection. The release of multiple virulence factors by *Xanthomonas* plantarum disrupts the host's defense system, enhances bacterial pathogenicity, and facilitates the infection of crops by pathogenic bacteria, leading to the development of plant diseases.[56] Bacterial pathogenicity can be measured as the strength of bacterial virulence at the *in vivo* level. Thus, the pathogenicity of bacteria depends on their ability to secrete virulence factors. All previous *in vitro* experiments showed that the compound THC could effectively inhibit the virulence factors of *Xoo*, however, it has not been confirmed in *in vivo* experiments, so the corresponding *in vivo* pathogenicity validation experiments were carried out. The results, as shown in Fig. 5, showed that compound THC at the different dose of 0 μg mL^{-1}, TC-100 μg mL^{-1}, and THC-100 μg mL^{-1} resulted in spot lengths of 11.0 cm, 9.2 cm, and 3.1 cm for rice leaf blight, respectively. Therefore, these results of *in vivo* pathogenicity experiments in rice indicate that compound THC can effectively reduce the pathogenicity of rice bacterial leaf blight at an early *in vivo* level.

3.5. The assay of THC against rice bacterial leaf blight

The alkaloid THC showed good biological activity against *Xoo in vitro* and exhibited fascinating anti-biofilm functions. Effective control of rice leaf blight *in vivo* is our ultimate goal. Therefore, *in vivo* control experiments of rice leaf blight were executed. The results of the experiment were shown in Fig. 6 and Table 2, THC showed good therapeutic efficacy with a control effect of 32.5%, which was slightly higher than that of the commercial drug thiabendazole (30.0%).

3.6. The assay of THC and 0.3% OPO against rice bacterial leaf blight

Although the therapeutic activity of THC was evaluated in Fig. 6, it was generally effective. However, we wanted to find an effective pesticide additive to enhance the therapeutic activity of THC. Pesticide additives have various functions, such as reducing the surface tension of the liquid to make the liquid spread quickly, increasing the droplet adhesion, enhancing the affinity between the liquid and the waxy leaf surface, strengthening the penetration effect, enlarging the contact area of the liquid, and enhancing the adhesion rate of the liquid on the leaf surface. Based on previous research, OPO is a widely used pesticide additive derived from natural plant essential oils.[57] As

Fig. 7 The curative activity of THC and 0.3% OPO against *Xoo* at 0 μg mL^{-1} (served as CK), and THC-200 μg mL^{-1}.

© 2025 The Author(s). Published by the Royal Society of Chemistry

Open Access Article. Published on 24 December 2025. Downloaded on 2/3/2026 5:24:52 AM.
This article is licensed under a Creative Commons Attribution-NonCommercial 3.0 Unported Licence.

Table 3 Curative activity of THC and 0.3% OPO against *Xoo* under greenhouse conditions at 200 μg mL^{-1} *in vivo*

	Curative activity		
Treatment	Morbidity	Disease index	Control efficiency[b]
THC + 0.3% OPO	100%	51.1%	42.5%
CK[a]	100%	89.0%	—

[a] Control. [b] Statistical analysis was performed using ANOVA under condition of equal variances assumed ($p < 0.05$).

shown in Fig. 7 and Table 3, the contact angle of water on the surface of rice leaves was 110° at a dose of 200 μg mL^{-1}. The contact angle of water on the surface of rice leaves was 110°. The contact angle of THC containing 0.3% essential oil of orange peel on the surface of rice leaf was 53°, and the therapeutic efficacy was 42.5%, which was significantly enhanced by 10%. The results showed that orange peel essential oil is a good natural pesticide additive.

3.7. ADMET prediction and phytotoxicity assessment

Inadequate assessment of pharmacokinetic profiles of pesticide candidates along with imperfect evaluation of drug toxicity is a main cause of failure in the later stages of pesticide development. In this study, the absorption, distribution, metabolism, excretion, and toxicity (ADMET) characteristics of drugs was systematically evaluated using the ADMETlab 2.0 computational platform (accessed at https://admetmesh.scbdd.com, accessed on May 16, 2025).[58] As shown in Fig. 8A, the ADMET assessment functional module of the platform is built based on the multi-task graphical attention framework and contains a series of high-quality prediction models, which can efficiently calculate 17 physicochemical properties, 13 medicinal chemistry parameters, 23 ADME indicators, 27 toxicity endpoints,

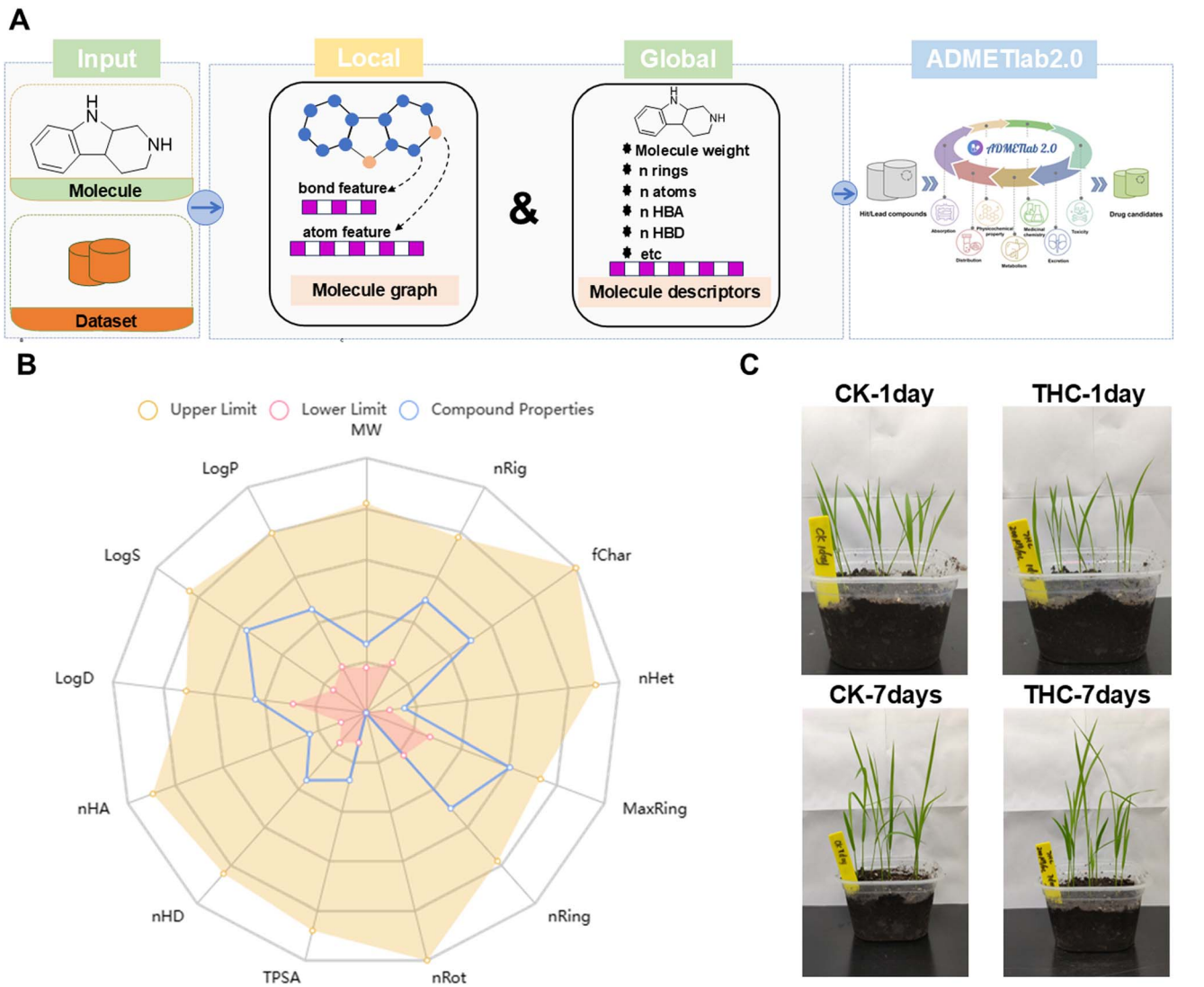

Fig. 8 (A) The fundamental framework of the ADMETlab assessment. (B) The physicochemical property of THC. (C) Phytotoxicity assessment of THC at the concentrations of 200 μg mL^{-1}.

© 2025 The Author(s). Published by the Royal Society of Chemistry

Open Access Article. Published on 24 December 2025. Downloaded on 2/3/2026 5:24:52 AM. This article is licensed under a Creative Commons Attribution-NonCommercial 3.0 Unported Licence.

and 8 toxicity motif rules (including 751 sub-structures), and provide technical support for the screening of promising lead compounds. Fig. 8B and Table S1 show that THC exhibits good pharmacological and toxicological properties, with good results in synthetic accessibility score, Fsp3, medicinal chemistry evolution (MCE-18), Lipinski rule, Pfizer rule, Pfizer rule, and Pfizer rule. Rule, Pfizer rule, GSK rule, Caco-2 permeability, MDCK permeability, Pgp-inhibitor, Pgp-substrate, Human Intestinal Absorption (HIA), F (20%): 20%. Bioavailability, F (30%): 30% Bioavailability, Plasma Protein Binding (PPB), Volume Distribution (VD), the fraction unbound in plasms (Fu), Clearance (CL), the human Ether-à-go-go-Related Gene Blockers (hERG Blockers), Drug Induced Liver Injury (DILI), Carcinogen city, eye corrosives, eye irritation, *etc.* The results of Fig. 8C showed that the growth of rice seedlings was not significantly inhibited seven days after spraying THC at a concentration of 200 μg mL^{-1}. Similarly, the phytotoxicity of THC derivatives has primarily been assessed in mature rice plants and it exhibited low phytotoxicity.[59] The comprehensive evaluation showed that THC has good ADMET properties and is expected to be developed as a new green pesticide for the control of rice leaf blight.

4. Conclusions

In conclusion, as an important commercial insecticide, THC has good therapeutic control of *Xoo*-induced rice leaf blight. Meanwhile, few studies have been reported on the control of rice leaf blight by THC and its antimicrobial mechanism. In our study, we investigated in detail the antimicrobial mechanism and control effect of THC against rice leaf blight bacteria. The results showed that THC possessed good therapeutic activity (32.5–42.5%) and excellent antibiofilm activity. These results of ADMET and phytotoxicity experiments indicated that THC was safer for target crops, and it was expected to be a novel green bactericide targeting biofilm.

Author contributions

Conceptualization, P. Q. and L. S.; methodology, P. Q. and L. S.; software, P. Q. and L. S.; formal analysis, H. L. and Y. L.; data curation, P. Q. and L. S.; writing—original draft preparation, P. Q. and L. S.; writing—review and editing, P. Q.; visualization, D. T., L. S., J. W., and Q. Z.; supervision, T. J., S. J., F. W., Y. G., Y. W., and L. L.; project administration, L. S. and J. S.; funding acquisition, L. S. and J. S. All authors have read and agreed to the published version of the manuscript.

Conflicts of interest

The authors declare no conflicts of interest.

Data availability

The original contributions presented in this study are included in this article; further inquiries can be directed to the corresponding authors.

Supplementary information: Table S1. ADMETlab assessment. Fig. S1. The antibacterial activity of four THC analogues and thiodiazole-copper against Xoo. See DOI: https://doi.org/10.1039/d5ra07526b.

Acknowledgements

We acknowledge the support from the Scientific Research Foundation of Guiyang Healthcare Vocational University (Guiyang Healthcare Vocational University, No.: Guikangda K2024-5, K2024-6, K2024-9, K2025-001) and Guizhou Province [Qianjiaoji (2022)400]; Guizhou Province [Qiankehe (2024)148]; Guiyang City Science and Technology Plan Project (No. [2024]2-36); Guizhou Province [Qiankehe (2025)015], Guizhou Province Science and Technology Innovation Leading Talent Workstation of Solid Functional Materials (KXJZ[2024]015).

References

1 Y. Q. Huang, Z. L. Guo, H. J. Song, Y. X. Liu, L. Z. Wang and Q. M. Wang, *J. Agric. Food Chem.*, 2018, **66**, 8253–8261.
2 V. A. Barbosa, P. Baréa, R. S. Mazia, T. Ueda-Nakamura, W. Ferreira da Costa, M. Ann Foglio, A. L. T. Goes Ruiz, J. E. de Carvalho, D. B. Vendramini-Costa, C. V. Nakamura and M. H. Sarragiotto, *Eur. J. Med. Chem.*, 2016, **124**, 1093–1104.
3 S. Rahul, J. Aanchal, K. M. Indresh and B. S. Deepak, *Bioorg. Med. Chem. Lett.*, 2020, **30**, 126869.
4 S. F. Li, K. Zhang, Y. Y. Chen, Z. B. Li, Q. B. Hu and Q. F. Weng, *Int. J. Fruit Sci.*, 2022, **22**, 646–663.
5 V. J. Glick, C. A. Webber, L. E. Simmons, M. C. Martin, M. Ahmad, C. H. Kim, A. N. D. Adams, S. Bang, M. C. Chao, N. C. Howard, S. M. Fortune, M. Verma, M. Jost, L. K. Beura, M. J. James, S. Y. Lee, C. M. Mitchell, J. Clardy, K. H. Kim and S. Gopinath, *Cell Host Microbe*, 2024, **32**, 1897–1909.
6 F. Hadjaz, S. Besret, F. Martin-Nizard, S. Yous, S. Dilly, N. Lebegue, P. Chavatte, P. Duriez, P. Berthelot and P. Carato, *Eur. J. Med. Chem.*, 2011, **46**, 2575–2585.
7 L. T. D. Tonin, V. A. Barbosa, C. C. Bocca, É. R. F. Ramos, C. V. Nakamura, W. F. da Costa, E. A. Basso, T. U. Nakamura and M. H. Sarragiotto, *Eur. J. Med. Chem.*, 2009, **44**, 1745–1750.
8 H. W. Liu, Q. T. Ji, G. G. Ren, F. Wang, F. Su, P. Y. Wang, X. Zhou, Z. B. Wu, Z. Li and S. Yang, *J. Agric. Food Chem.*, 2020, **68**, 12558–12568.
9 A. W. Hummel, K. E. Wilkins, L. Wang, R. A. Cernadas and A. J. Bogdanove, *Mol. Plant Pathol.*, 2016, **18**, 55–66.
10 X. Y. Pan, S. Xu, J. Wu, J. Y. Luo, Y. B. Duan, J. X. Wang, F. Zhang and M. G. Zhou, *Pestic. Biochem. Physiol.*, 2018, **145**, 8–14.
11 P. M. Ebling and S. B. Holmes, *Pest Manag. Sci.*, 2002, **58**, 1216–1222.
12 X. Lv, M. T. Yuan, Y. H. Pei, C. Y. Liu, X. C. Wang, L. Wu, D. Q. Cheng, X. Z. Ma and X. C. Sun, *J. Agric. Food Chem.*, 2021, **69**, 4992–5002.

© 2025 The Author(s). Published by the Royal Society of Chemistry

Open Access Article. Published on 24 December 2025. Downloaded on 2/3/2026 5:24:52 AM. This article is licensed under a Creative Commons Attribution-NonCommercial 3.0 Unported Licence.

13 A. M. T. Barnes, J. L. Dale, Y. Chen, D. A. Manias, K. E. Greenwood Quaintance, M. K. Karau, P. C. Kashyap, R. Patel, C. L. Wells and G. M. Dunny, *Virulence*, 2016, **8**, 282–296.
14 N. P. Caires, L. M. S. Guimarães, P. S. Hermenegildo, F. A. Rodrigues, J. L. Badel and A. C. Alfenas, *Plant Pathol.*, 2020, **69**, 549–558.
15 O. Ciofu and T. Tolker-Nielsen, *Front. Microbiol.*, 2019, **10**, 913.
16 R. Ramakrishnan, A. K. Singh, S. Singh, D. Chakravortty and D. Das, *J. Biol. Chem.*, 2022, **298**, 102352.
17 M. Elafify, X. y. Liao, J. s. Feng, J. Ahn and T. Ding, *Food Res. Int.*, 2024, **190**, 114650.
18 W. Hao, Q. C. Li, P. P. Liu, J. B. Han, R. Duan and P. Liang, *Sci. Total Environ.*, 2022, **823**, 153657.
19 H. Gu, S. W. Lee, J. Carnicelli, Z. W. Jiang and D. C. Ren, *J. Bacteriol.*, 2019, **201**, e00034.
20 Y. Z. Li, X. Li, Y. Hao, Y. Liu, Z. L. Dong and K. X. Li, *Int. J. Biol. Sci.*, 2021, **17**, 1769–1781.
21 J. F. Wang, Q. J. Liu, D. Y. Dong, H. D. Hu, B. Wu and H. Q. Ren, *Environ. Int.*, 2020, **140**, 105722.
22 E. M. Hetrick, J. H. Shin, H. S. Paul and M. H. Schoenfisch, *Biomaterials*, 2009, **30**, 2782–2789.
23 H. J. Busscher and H. C. van der Mei, *Clin. Microbiol. Rev.*, 2006, **19**, 127–141.
24 W. y. Cai, J. f. Wu, C. w. Xi and M. E. Meyerhoff, *Biomaterials*, 2012, **33**, 7933–7944.
25 M. C. Gagliano, T. R. Neu, U. Kuhlicke, D. Sudmalis, H. Temmink and C. M. Plugge, *Front. Microbiol.*, 2018, **9**, 1423.
26 M. Khider, E. Hjerde, H. Hansen and N. P. Willassen, *BMC Genom.*, 2019, **20**, 220.
27 M. F. Moradali, S. Ghods and B. H. A. Rehm, *Front. Cell. Infect. Microbiol.*, 2017, **7**, 39.
28 O. E. Petrova and K. Sauer, *J. Bacteriol.*, 2012, **194**, 2413–2425.
29 C. T. Nguyen, S. R. Robinson, W. Jung, M. A. Novak, S. A. Boppart and J. B. Allen, *Hear. Res.*, 2013, **301**, 193–200.
30 H. Qian, W. Li, L. X. Guo, L. Tan, H. Q. Liu, J. J. Wang, Y. J. Pan and Y. Zhao, *Front. Microbiol.*, 2020, **11**, 23.
31 J. C. N. Fong and F. H. Yildiz, *J. Bacteriol.*, 2007, **189**, 2319–2330.
32 I. Heuschkel, R. Dagini, R. Karande and K. Bühler, *Front. Bioeng. Biotechnol.*, 2020, **8**, 588729.
33 N. G. Cogan, J. Li, S. Fabbri and P. Stoodley, *Biophys. J.*, 2018, **115**, 1393–1400.
34 L. Kvich, M. Burmølle, T. Bjarnsholt and M. Lichtenberg, *Front. Cell. Infect. Microbiol.*, 2020, **10**, 396.
35 P. Y. Qi, T. H. Zhang, Y. M. Feng, M. W. Wang, W. B. Shao, D. Zeng, L. H. Jin, P. Y. Wang, X. Zhou and S. Yang, *J. Agric. Food Chem.*, 2022, **70**, 4899–4911.
36 J. Yang, H. J. Ye, H. M. Xiang, X. Zhou, P. Y. Wang, S. S. Liu, B. X. Yang, H. B. Yang, L. W. Liu and S. Yang, *Adv. Funct. Mater.*, 2023, 2303206, DOI: 10.1002/adfm.202303206.
37 P. Y. Qi, L. H. Shi, Z. C. Zheng, Y. M. Feng, T. H. Zhang, R. S. Luo, S. Tan, A. L. Tang, H. Y. Huang, X. Zhou, H. M. Xiang, L. W. Liu and S. Yang, *Carbohydr. Polym.*, 2025, **363**, 123733.
38 T. H. Zhang, Y. K. Yang, Y. M. Feng, Z. J. Luo, M. W. Wang, P. Y. Qi, D. Zeng, H. W. Liu, Y. M. Liao, J. Meng, X. Zhou, L. W. Liu and S. Yang, *Pest Manag. Sci.*, 2024, **81**, 585–598.
39 L. W. Liu, Z. H. Ding, G. G. Ren, G. D. Wang, X. Pan, G. H. Wei, X. Zhou, Z. B. Wu, Z. C. Jin, Y. g. Robin Chi and S. Yang, *Chem. Eng. J.*, 2023, **475**, 146041.
40 P. L. Chu, Y. M. Feng, Z. Q. Long, W. L. Xiao, J. Ji, X. Zhou, P. Y. Qi, T. H. Zhang, H. Zhang, L. W. Liu and S. Yang, *J. Agric. Food Chem.*, 2023, **71**, 6525–6540.
41 X. Zhou, Y. H. Fu, Y. Y. Zou, J. Meng, G. P. OuYang, Q. S. Ge and Z. C. Wang, *Int. J. Mol. Sci.*, 2022, **23**, 12365.
42 A. Yepes, J. Schneider, B. Mielich, G. Koch, J. C. García-Betancur, K. S. Ramamurthi, H. Vlamakis and D. López, *Mol. Microbiol.*, 2012, **86**, 457–471.
43 W. Pan, M. Fan, H. Wu, C. Melander and C. Liu, *J. Appl. Microbiol.*, 2015, **119**, 1403–1411.
44 E. Cremonini, E. Zonaro, M. Donini, S. Lampis, M. Boaretti, S. Dusi, P. Melotti, M. M. Lleo and G. Vallini, *Microb. Biotechnol.*, 2016, **9**, 758–771.
45 W. Kuephadungphan, A. P. G. Macabeo, J. J. Luangsa-ard, K. Tasanathai, D. Thanakitpipattana, S. Phongpaichit, K. Yuyama and M. Stadler, *Mycol. Prog.*, 2018, **18**, 135–146.
46 V. Donato, F. R. Ayala, S. Cogliati, C. Bauman, J. G. Costa, C. Leñini and R. Grau, *Nat. Commun.*, 2017, **8**, 14332.
47 G. F. Liang, H. Shi, Y. J. Qi, J. H. Li, A. H. Jing, Q. W. Liu, W. P. Feng, G. D. Li and S. G. Gao, *Int. J. Nanomed.*, 2020, **15**, 5473–5489.
48 M. A. Hassani, P. Durán and S. Hacquard, *Microbiome*, 2018, **6**, 58.
49 V. Kontham, B. Ippakayala and D. Madhu, *Arabian J. Chem.*, 2021, **14**, 103163.
50 P. J. Buch, Y. Chai and E. D. Goluch, *Clin. Microbiol. Rev.*, 2019, **32**, e00091–00018.
51 J. Yao and C. Allen, *J. Bacteriol.*, 2006, **188**, 3697–3708.
52 M. Theves, J. Taktikos, V. Zaburdaev, H. Stark and C. Beta, *Biophys. J.*, 2013, **105**, 1915–1924.
53 F. Seijsing, L. Nileback, O. Ohman, R. Pasupuleti, C. Stahl, J. Seijsing and M. Hedhammar, *MicrobiologyOpen*, 2020, **9**, e993.
54 G. H. Wu, J. Majewski, C. Ege, K. Kjaer, M. J. Weygand and K. Y. C. Lee, *Biophys. J.*, 2005, **89**, 3159–3173.
55 M. Chen, H. Sun, M. Boot, L. Shao, S. J. Chang, W. w. Wang, T. T. Lam, M. Lara-Tejero, E. H. Rego and J. E. Galán, *Sci. Educ.*, 2020, **369**, 450–455.
56 N. Bae, H. J. Park, H. Park, M. y. Kim and S. W. Han, *Mol. Plant Pathol.*, 2018, **19**, 2527–2542.
57 L. H. Shi, X. Zhou and P. Y. Qi, *Molecules*, 2024, **29**, 4297.
58 S. S. Liu, D. Zeng, T. H. Zhang, J. H. Hu, B. X. Yang, J. Yang, X. Zhou, P. Y. Wang, L. W. Liu, Z. B. Wu and S. Yang, *Eur. J. Med. Chem.*, 2023, **250**, 115215.
59 Y. K. Yang, S. S. Su, Z. J. Sun, Z. Q. Long, X. C. Fu, J. Meng, X. Zhou, L. W. Liu and S. Yang, *Bioorg. Chem.*, 2025, **160**, 108473.

© 2025 The Author(s). Published by the Royal Society of Chemistry